Effect of spin diffusion on Gilbert damping for a very thin permalloy layer in Cu/permalloy/Cu/Pt films

S. Mizukami,* Y. Ando, and T. Miyazaki
Department of Applied Physics, Graduate School of Engineering, Tohoku University, Aoba-yama 05, Sendai, Japan
(Received 11 March 2002; revised manuscript received 18 June 2002; published 16 September 2002)

Ferromagnetic resonance (FMR) was measured for Cu/permalloy (Py) (20, 30, 40 Å)/Cu (d_{Cu})/Pt (0, 50 Å) films with various d_{Cu} to clarify the effect of spin diffusion driven by the precession of magnetization on Gilbert damping. The peak-to-peak linewidth ΔH_{pp} of the FMR spectra for Cu/Py/Cu/Pt films was very large at $d_{Cu}=0$ Å, and decreased remarkably at $d_{Cu}=30$ Å. Above $d_{Cu}=30$ Å, it decreased gradually with increasing d_{Cu} in the anomalously wide range of d_{Cu}. The out-of-plane angular dependence of the FMR of Cu/Py(30 Å)/Cu (d_{Cu})/Pt (0, 50 Å) films was measured and analyzed using a Landau-Lifshitz-Gilbert equation that took into account the local variation of the effective demagnetizing field. The Gilbert damping coefficient G obtained from the analysis for Cu/Py/Cu/Pt films was about twice as large as that for Cu/Py/Cu films even at $d_{Cu}=100$ Å and decreased gradually as d_{Cu} increased. At $d_{Cu}=2000-3000$ Å, G for Cu/Py/Cu/Pt and Cu/Py/Cu films has the same value. We discussed the influence of spin diffusion driven by the precession of magnetization in FMR on G using a previously proposed model. The calculated G vs d_{Cu} fitted well to the experimental one, and the other features of the experimental results are well explained by the model.

DOI: 10.1103/PhysRevB.66.104413 PACS number(s): 75.70.−i, 76.50.+g, 72.25.Mk, 72.25.Rb

I. INTRODUCTION

Recently, it has been predicted theoretically that a spin-polarized current can excite spin wave or drive the reversal of magnetization in a very thin ferromagnetic metal (FM) layer involved in a FM/normal metal (NM)/FM film.[1,2] Many groups have examined the prediction experimentally,[3] as it is expected to be applicable to magnetoelectronics, such as the magnetic random access memory.[2] Furthermore, Berger has suggested that the inverse effects can also appear in FM/NM/FM films, such as spin accumulation induced by the precession of magnetization in the ferromagnetic resonance (FMR).[1,4] For a full understanding of the effects of spin-polarized current on the dynamics of magnetization, study of such inverse effects is important.

A similar inverse effect has been studied in FM/NM bilayers using conduction-electron spin resonance (CESR) combined with FMR.[5–7] Silsbee *et al.* suggested that the precession of magnetization for a FM layer can drive conduction spin diffusion at the FM/NM interface.[6] If the thickness of the FM layer is sufficiently thin, it can be expected that spin diffusion driven by the precession of magnetization in FMR also influences the dynamics of magnetization for the FM layer, particularly the magnetic damping, in a NM/FM/NM film. Intrinsic magnetic damping, so-called Gilbert damping, has been extensively investigated for bulk or FM film using measurements of the linewidth and the line shape of FMR spectrum,[8,10,9,11] while no studies of a similar nature have been reported of Gilbert damping for a thin FM layer.

To clarify the effect of spin diffusion on Gilbert damping for a very thin FM layer, we studied the linewidth of FMR for a thin $Ni_{80}Fe_{20}$ permalloy (Py) layer in NM/Py/NM films (NM=Cu, Ta, Pd, and Pt).[12,13] In this study, it has been found that Gilbert damping coefficient G increased when NM=Pt or Pd, and was almost unchanged for NM=Cu or Ta. For bulk FM, the magnitude of G is considered to depend on that of the spin-orbit coupling,[14] so it is unclear whether spin diffusion is responsible for the enhancement of G for Pt/Py/Pt or Pd/Py/Pd films. Therefore, we studied the linewidth of FMR for Cu/Py/Cu/Pt films with various Cu spacer layer thicknesses to examine the effect of spin diffusion on G for a very thin Py film. The experimental results have already been briefly reported.[15] In this paper, we describe the experimental data in detail and discuss G for Cu/Py/Cu/Pt films using the phenomenological model proposed by Silsbee *et al.*[6]

II. EXPERIMENTAL PROCEDURE

Films were prepared by magnetron sputtering on the substrate of Corning 7059 glass cooled by water. The base pressure was less than 5×10^{-7} Torr, and Ar pressure was 7 mTorr. Cu/Py (d_{Py})/Cu (d_{Cu})/Pt (50 Å) films were systematically fabricated with varying d_{Py} and d_{Cu}. We also fabricated Cu/Py (d_{Py})/Cu (d_{Cu}) films and Cu/Py (d_{Py})/Cu (50 Å)/Cu (50 Å)/Pt (50 Å) films as control samples. In fabricating Cu/Py (d_{Py})/Cu (50 Å)/Cu (50 Å)/Pt (50 Å) films, the films were exposed to air after sputtering the first 50 Å Cu spacer layer. In addition, Cu/Py (30 Å)/Cu (100 Å)/Pt (d_{Pt})/Cu (50 Å) films were also prepared with various d_{Pt}. The thickness of the Cu buffer layer was 50 Å for all samples. FMR was measured using a *X*-band (9.77 GHz) electron-spin-resonance spectrometer and a TE 102 cavity. For measurements of the out-of-plane angular dependence of FMR, the sample was fixed on a quartz rod, and a goniometer was used to vary the angle. Magnetization measurements were carried out by a superconducting quantum interference device magnetometer. The surface morphology of the films was measured using an atomic force microscope.

III. METHOD OF ANALYSIS OF THE OUT-OF-PLANE ANGULAR DEPENDENCE OF FMR

The linewidth of FMR reflects not only G but also the magnetic inhomogeneities in a film, such as the local varia-

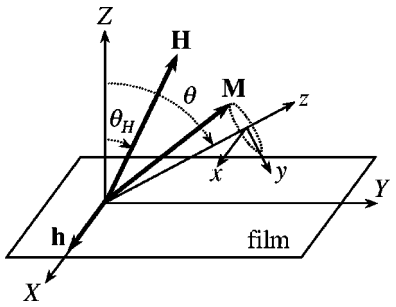

FIG. 1. The coordinate system used for measurement and analysis of the out-of-plane angular dependence of FMR.

tion of magnetic anisotropy, the so-called anisotropy dispersion. In order to evaluate G for the films from the linewidth of FMR, we carried out measurements and numerical analyses of the out-of-plane angular dependence of FMR,[16,17,11–13] which is based on the Landau-Lifshitz-Gilbert (LLG) equation,[8]

$$-\frac{1}{\gamma}\frac{d\mathbf{M}}{dt}=\mathbf{M}\times(\mathbf{H}_{\rm eff}+\mathbf{h})-\frac{\alpha}{\gamma M_S}\mathbf{M}\times\frac{d\mathbf{M}}{dt}. \tag{1}$$

Here $\mathbf{M}$, $\mathbf{H}_{\rm eff}$, $\mathbf{h}$, and M_S are the vectors of the magnetization, the effective magnetic field acting on $\mathbf{M}$, the external microwave field, and the saturation magnetization, respectively. γ and α are the gyromagnetic ratio and the dimensionless damping coefficient, defined as $\gamma\equiv g\mu_B/\hbar$ and $\alpha\equiv G/\gamma M_S$, respectively. Here, g, μ_B, and $\hbar$ are the g factor, the Bohr magneton number, and the Planck constant, respectively. We took into account the external dc magnetic field, the demagnetizing field, and the perpendicular anisotropy field as $\mathbf{H}_{\rm eff}$. The coordinate system is as in Fig. 1. The vector of the external dc magnetic field $\mathbf{H}$ lies in the Y-Z plane, and its direction is defined by θ_H. $\mathbf{h}$ is parallel to the X direction and is written as

$$\mathbf{h}=\delta h e^{-i\omega t}\hat{\mathbf{X}}. \tag{2}$$

Here, $\omega=2\pi f$, and f is the microwave frequency. The small precession of $\mathbf{M}$ around the equilibrium direction is taken as a solution of Eq. (1), which is given as

$$\mathbf{M}=\delta M_x e^{-i\omega t}\hat{\mathbf{x}}+\delta M_y e^{-i\omega t}\hat{\mathbf{y}}+M_S\hat{\mathbf{z}}. \tag{3}$$

Here, the z axis is taken to be the equilibrium direction defined by θ. The y-z plane lies in the Y-Z plane, and the x axis is identical to the X axis. Substituting Eqs. (2) and (3) into Eq. (1), one obtains the resonance condition of the FMR on the linear approximation, which is given by the following relations,[16,12]

$$\omega/\gamma=\sqrt{H_1H_2}, \tag{4}$$

$$H_1=H_{res}\cos(\theta_H-\theta)-4\pi M_{\rm eff}\cos 2\theta, \tag{5}$$

$$H_2=H_{res}\cos(\theta_H-\theta)-4\pi M_{\rm eff}\cos^2\theta. \tag{6}$$

Here, H_{res} is the resonance field and $4\pi M_{\rm eff}$ is the effective demagnetizing field defined as $4\pi M_{\rm eff}\equiv 4\pi M_S-2K_\perp/M_S$, with the perpendicular magnetic anisotropy constant $K_\perp$. θ is obtained from the following equation:

$$2H_{res}\sin(\theta-\theta_H)=4\pi M_{\rm eff}\sin 2\theta. \tag{7}$$

One also obtains the full width at half maximum (FWHM) of a FMR spectrum caused intrinsically by Gilbert damping from Eq. (1), which is expressed as[16,12]

$$\Delta H_{\rm in}=\alpha(H_1+H_2)\left|\frac{d(\omega/\gamma)}{dH_{res}}\right|^{-1}. \tag{8}$$

We assume that the FWHM due to the anisotropy dispersion for the out-of-plane direction is expressed as[17,11,12]

$$\Delta H_{\rm ex}=\left|\frac{dH_{res}}{d(4\pi M_{\rm eff})}\right|\Delta(4\pi M_{\rm eff})+\left|\frac{dH_{res}}{d\theta_H}\right|\Delta\theta_H. \tag{9}$$

Here, $\Delta(4\pi M_{\rm eff})$ and $\Delta\theta_H$ represent the dispersion of the magnitude and the direction of $4\pi M_{\rm eff}$, respectively. Equation (9) states that the extrinsic linewidth $\Delta H_{\rm ex}$ is caused by the local variation of the magnitude and the direction of $4\pi M_{\rm eff}$ through the local variation of H_{res}. The influence of the anisotropy dispersion parallel to a film plane on $\Delta H_{\rm ex}$ is not taken into account since it is considered to be small for Py films.[18] The peak-to-peak linewidth ΔH_{pp} is assumed to be expressed as[17,11,12]

$$\Delta H_{pp}=\Delta H_{\rm in}/\sqrt{3}+\Delta H_{\rm ex}/\sqrt{3}. \tag{10}$$

Here, the multiplying of $1/\sqrt{3}$ is the correction of the difference between the FWHM and the peak-to-peak linewidth for the line shape of Lorentzian. H_{res} vs θ_H is calculated using Eqs. (4)–(7) numerically, and is fitted to the experimental H_{res} vs θ_H by adjusting the value of g and $4\pi M_{\rm eff}$. ΔH_{pp} vs θ_H is also calculated from Eqs. (4)–(10) numerically, using g and $4\pi M_{\rm eff}$ obtained from the fitting of H_{res} vs θ_H, and is fitted to the experimental ΔH_{pp} vs θ_H by adjusting the value of α, $\Delta(4\pi M_{\rm eff})$, and $\Delta\theta_H$. It is noted that the multiplying of $1/\sqrt{3}$ for the second term of Eq. (10) has been omitted in other papers.[11,17] Since the spectra for our films were Lorentzian except for $\theta_H\simeq 0°$, we assumed the multiplying of $1/\sqrt{3}$. However, the value of α evaluated from the fitting does not depend on this assumption.

IV. EXPERIMENTAL RESULTS

Figure 2(a) shows the examples of FMR spectra measured at $\theta_H=90°$ for Cu/Py (30 Å)/Cu ($d_{\rm Cu}$)/Pt films with various $d_{\rm Cu}$. The spectra are normalized and are shown as a function of the external dc magnetic field around H_{res}. Although the spectra for $d_{\rm Cu}=0$ and 30 Å are slightly asymmetric, the spectra keep the line shape of a Lorentzian for all $d_{\rm Cu}$. Figure 2(b) shows the spectra for Cu/Py (30 Å)/Cu (100 Å)/Pt and Cu/Py (30 Å)/Cu (100 Å) films in the same manner as that in Fig. 2(a). The calculated Lorentzian curves are shown in Fig. 2(b) with the solid lines. Lorentzian curves fit the experimental data almost completely for both the films. It is unlikely that the difference of ΔH_{pp} between the films with and without the Pt layer is due to the increase of anisotropy dispersion in a film, because if the anisotropy dispersion

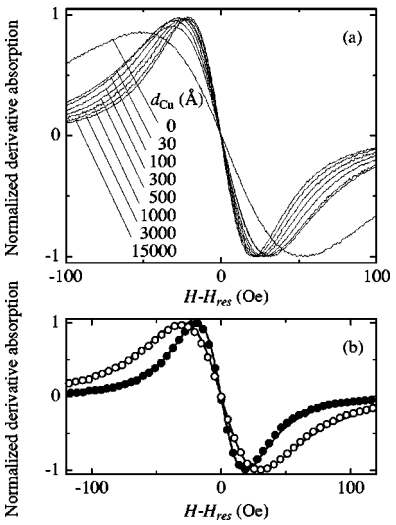

FIG. 2. (a) Normalized FMR spectra measured at $\theta_H = 90°$ for Cu/Py (30 Å)/Cu (d_{Cu})/Pt films with various d_{Cu}. Horizontal axis is the external dc magnetic field measured from H_{res}. (b) Normalized FMR spectra measured at $\theta_H = 90°$ for Cu/Py (30 Å)/Cu (100 Å)/Pt film (open circles) and Cu/Py (30 Å)/Cu (100 Å) film (solid circles). Lines are the calculated Lorentzian curves and are fitted to the experimental data. The experimental data points are thinned for easier viewing.

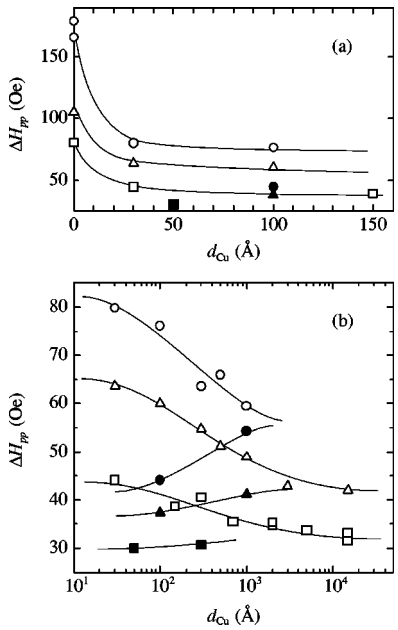

FIG. 3. d_{Cu} dependence of the peak-to-peak linewidth ΔH_{pp} (a) in the thinner regime of d_{Cu} and (b) in the full range of d_{Cu} for Cu/Py (d_{Py})/Cu (d_{Cu})/Pt (d_{Pt}) films. Data were obtained from the FMR spectra measured at $\theta_H = 90°$. The open and the solid symbols correspond to the data for $d_{Pt} = 50$ and 0 Å, respectively. ○ (●), ▲ (△), and ■ (□) represent the data for $d_{Py} = 20$, 30, and 40 Å, respectively. Lines are visual guides.

were to increase ΔH_{pp} dominantly through the local variation of H_{res}, the line shape would tend to become Gaussian-like or a heavily distorted line shape.[19] In addition, we note that the shapes of the magnetization curves for these films are same.

Figures 3(a) and 3(b) show d_{Cu} dependence of ΔH_{pp} for Cu/Py (d_{Py})/Cu (d_{Cu})/Pt (0,50 Å) films with various d_{Py} in the thinner regime of d_{Cu} and in the full range of d_{Cu}, respectively. ΔH_{pp} was obtained from the FMR spectra measured at $\theta_H = 90°$. As seen in Fig. 3(a), ΔH_{pp} for Cu/Py/Cu/Pt film is rather large at $d_{Cu} = 0$ Å. Such a large ΔH_{pp} has also been observed for Pt/Py/Pt film.[12,13] By inserting a 30 Å thick Cu spacer layer, ΔH_{pp} drops remarkably, implying that the large increase of ΔH_{pp} requires the intimate contact of the Pt layer. While, ΔH_{pp} for Cu/Py/Cu/Pt film is still larger than that for the films without the Pt layer, and decreases gradually for a wide range of d_{Cu}, as shown in Fig. 3(b), ΔH_{pp} for Cu/Py/Cu films increases slightly with increasing d_{Cu}. ΔH_{pp} for the films with and without the Pt layer becomes almost the same at $d_{Cu} = 2000$–3000 Å. With decreasing d_{Py}, the difference of ΔH_{pp} between those films increases in the thin regime of d_{Cu}. On the other hand, H_{res} is independent of d_{Cu} and is not influenced by the Pt layer.

Figure 4 shows ΔH_{pp} for Cu/Py (30 Å)/Cu (100 Å)/Pt (d_{Pt})/Cu films as a function of d_{Pt}. ΔH_{pp} was obtained from the FMR spectra measured at $\theta_H = 90°$. ΔH_{pp} increases rapidly in the very thin regime of d_{Pt} and saturates at $d_{Pt} \simeq 10$ Å. This thickness is supposedly the thickness at which the Pt islands become a continuous layer and entirely cover the surface of the Cu layer. This result implies that the increase of ΔH_{pp} for Cu/Py/Cu/Pt film requires only the interface between the Cu and the Pt layer.

We measured the out-of-plane angular dependence of FMR for Cu/Py (30 Å)/Cu (d_{Cu})/Pt (0, 50 Å) films. Figures 5(a) and 5(b) show examples of the out-of-plane angular dependence of ΔH_{pp} and H_{res} for Cu/Py/Cu (100 Å) and Cu/Py/Cu (100 Å)/Pt films, respectively. ΔH_{pp} vs θ_H and H_{res} vs θ_H exhibit strong peaks at $\theta_H \simeq 15°$ and $\theta_H = 0°$, respectively. The peak of ΔH_{pp} at $\theta_H \simeq 15°$ is because of the increase of the linewidth due to Gilbert damping.[16,12,13] The peak of H_{res} at $\theta_H = 0°$ is caused by the demagnetizing field that is operatively strong at this angle. In the data of ΔH_{pp} vs θ_H for both films, another small peak is also found at $\theta_H = 0°$. This small peak is due to the dispersion of the magnitude of $4\pi M_{\text{eff}}$, which is also effective at this angle.[12,13,16] The data of H_{res} vs θ_H in the insets of Figs. 5(a) and 5(b) are nearly the same, indicating that g and $4\pi M_{\text{eff}}$ are same between the two films. On the other hand, ΔH_{pp} for Cu/Py/Cu (100 Å)/Pt film is larger than that for the film without the Pt

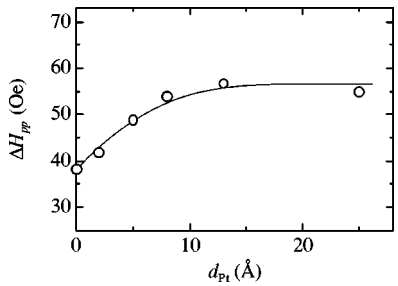

FIG. 4. d_{Pt} dependence of ΔH_{pp} for Cu/Py (30 Å)/Cu (100 Å)/Pt (d_{Pt})/Cu films. ΔH_{pp} was obtained from the FMR spectra measured at $\theta_H = 90°$. The line is a visual guide.

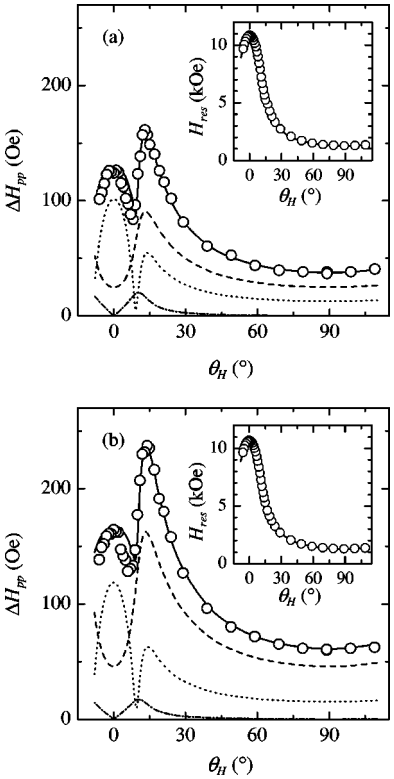

FIG. 5. The out-of-plane angular dependence of ΔH_{pp} for (a) Cu/Py (30 Å)/Cu (100 Å) and (b) Cu/Py (30 Å)/Cu (100 Å)/Pt film, respectively. Insets show the out-of-plane angular dependence of H_{res}. Open circles represent the experimental data. Solid lines are the calculated data and are fitted to the experimental ones. Broken, dotted, and dotted-and-broken lines are the three components of the calculated ΔH_{pp}. The best-fitted parameters are $g=2.11$, $4\pi M_{\rm eff}=7.5$ kG, $\alpha=0.0065$, $\Delta(4\pi M_{\rm eff})=175$ G, and $\Delta\theta_H=0.057°$ for Cu/Py (30 Å)/Cu (100 Å) and $g=2.11$, $4\pi M_{\rm eff}=7.4$ kG, $\alpha=0.012$, $\Delta(4\pi M_{\rm eff})=205$ G, and $\Delta\theta_H=0.052°$ for Cu/Py (30 Å)/Cu (100 Å)/Pt, respectively.

layer in the full range of θ_H. The increase of ΔH_{pp} in the full range of θ_H cannot be explained by two-magnon scattering, because the linewidth due to two-magnon scattering is zero around $\theta_H=0°$.[20] To our knowledge, such an increase of ΔH_{pp} is only explainable by the increasing of α.[12,13]

The experimental data of H_{res} vs θ_H and ΔH_{pp} vs θ_H were analyzed using the method described in Sec. III. The examples of the results of fitting are shown in Figs. 5(a) and 5(b) with the solid lines. The calculated data are well fitted to the experimental data for ΔH_{pp} and H_{res}. Three components of the calculated ΔH_{pp}, which are $\Delta H_{\rm in}/\sqrt{3}$ and the first and the second terms of $\Delta H_{\rm ex}/\sqrt{3}$, are shown in Figs. 5(a) and 5(b) with the broken, the dotted and the dotted-and-broken lines, respectively. The magnitudes of these three components of ΔH_{pp} are proportional to α, $\Delta(4\pi M_{\rm eff})$, and $\Delta\theta_H$ from Eqs. (8) and (9). Therefore, $\Delta(4\pi M_{\rm eff})$ and $\Delta\theta_H$ are almost the same between the two films, and only α is significantly different.

Analysis of the other films showed that only α systematically depended on $d_{\rm Cu}$ and the presence of the Pt layer. The value of g for these films was about 2.11, which agreed with

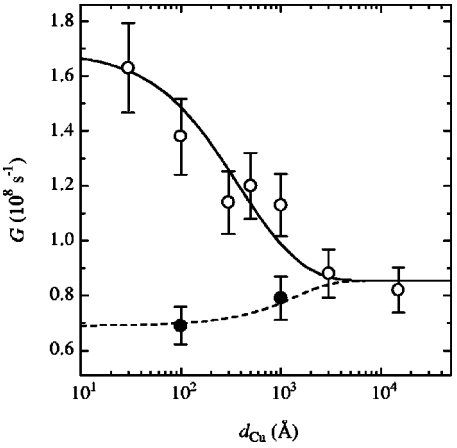

FIG. 6. $d_{\rm Cu}$ dependence of Gilbert damping coefficient G for Cu/Py (30 Å)/Cu ($d_{\rm Cu}$)/Pt films (open circle) and Cu/Py (30 Å)/Cu ($d_{\rm Cu}$) films (solid circle). Lines are the calculated data and are fitted to the experimental ones using Eqs. (25), (33), and (34) with $G_{\rm Py}=0.69\times10^8$ s^{-1}, $\chi_p=9.8\times10^{-7}$ (in cgs unit), $D_p=120$ cm^2/s, $l_p=2000$ Å, and $\Gamma=30$ cm/s. Solid and broken lines correspond to $\alpha_S^{-1}\rightarrow0$ and $\alpha_S=0$, respectively.

another reported value.[21] The value of $4\pi M_{\rm eff}$ was found to be about 7.5 kG. This value is almost same as the average value of $4\pi M_S\simeq7.2$ kG for these films, so that $K_\perp$ is negligible for the films, and this agrees with other reports.[22] No dependences of $\Delta(4\pi M_{\rm eff})$ or $\Delta\theta_H$ on $d_{\rm Cu}$ and the presence of the Pt layer are also reasonable findings, because $\Delta(4\pi M_{\rm eff})$ and $\Delta\theta_H$ for a thin Py layer are considered to be due to the local fluctuation of $d_{\rm Py}$ and the waviness of the Py layer,[12] and such structural imperfections cannot be influenced by an overlayer structure.

Figure 6 shows G for Cu/Py (30 Å)/Cu ($d_{\rm Cu}$)/Pt and Cu/Py (30 Å)/Cu ($d_{\rm Cu}$) films as a function of $d_{\rm Cu}$. The value of G was evaluated from α using g and M_S for each film. The errors in G are mostly due to the uncertainties of M_S. The trend of G for Cu/Py/Cu ($d_{\rm Cu}$)/Pt and Cu/Py/Cu ($d_{\rm Cu}$) films is similar to that of ΔH_{pp} shown in Fig. 3(b). In the thin region of $d_{\rm Cu}$, G for Cu/Py/Cu/Pt films is found to be about two times larger than that for films without the Pt layer. G for Cu/Py/Cu/Pt films decreases monotonically with increasing $d_{\rm Cu}$. G for Cu/Py/Cu films is close to the bulk value of G for Py in Ref. 23 at $d_{\rm Cu}=100$ Å and increases slightly as $d_{\rm Cu}$ increases. G for both films becomes equal at $d_{\rm Cu}=2000-3000$ Å.

V. DISCUSSION

The large ΔH_{pp} for Cu/Py/Pt films in Fig. 3(a) or G for Pt/Py/Pt films in Refs. 12 and 13 can be explained qualitatively by theories for Gilbert damping for bulk FM.[14] Similar explanations have been made for the enhancement of G in epitaxial Fe and Ni ultrathin films.[10,11] However, the rapid decrease of ΔH_{pp} in Fig. 3(a) implies that such an explanation is difficult for Cu/Py/Cu/Pt films, and some other mechanism should be taken into consideration for the explanation of the enhancement of G for these films. In discussing the mechanism of the enhancement of G for Cu/Py/Cu/Pt

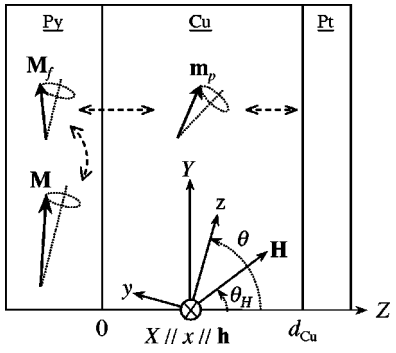

FIG. 7. A schematic illustration of the coordinate system used in the discussion.

films, we note that the enhancement of G was not observed for Cu/Py/Cu/Cu/Pt films. This means that the enhancement of G for Cu/Py/Cu/Pt films is caused by some mediation inside the Cu spacer layer. The mediation of the Ruderman-Kittel-Kasuya-Yosida–like spin polarization is excluded because it is known to be limited near the Py/Cu interface.[24] It is also difficult to consider that the enhancement of G is due to the pinholes or the diffusion of Pt atoms, because the Cu spacer layer is thick enough, and its surface is smooth from the AFM measurements. We consider that this long-range effect is related to the spin diffusion of the conduction electron in the Cu spacer layer, since the conduction electron can diffuse for a long distance in a Cu layer without losing its spin memory.[25,26] The spin diffusion can be driven by the precession of magnetization in FMR, as mentioned in Sec. I.[6] The enhancement of G for Cu/Py/Cu/Pt films is discussed from such a point of view, based on the phenomenological model proposed by Silsbee *et al.*[6]

The schematic illustration for this discussion is shown in Fig. 7. For simplicity, we neglect the effect of the Cu buffer layer. $\mathbf{M}$ is the vector of the magnetic moment per unit volume for the localized electron spins in the Py layer. $\mathbf{M}_f$ and $\mathbf{m}_p$ are those for the conduction-electron spins in the Py layer and the Cu layer, respectively. $\mathbf{H}$, $\mathbf{h}$, the X-Y-Z coordinate, and the x-y-z one are defined the same as those in Fig. 1. The dynamics of $\mathbf{M}$ are described by

$$-\frac{1}{\gamma_F}\frac{d\mathbf{M}}{dt}=\mathbf{M}\times(\mathbf{H}_{\rm eff}+\mathbf{h})-\frac{G_F}{(\gamma_F M_S)^2}\mathbf{M}\times\frac{d\mathbf{M}}{dt}+\mathbf{T}, \tag{11}$$

where γ_F is the gyromagnetic ratio and G_F is the Gilbert damping coefficient for the localized electron spins. We regard $\mathbf{M}$ and $\mathbf{H}_{\rm eff}$ to be the same as those in Eq. (1), since the magnetization M_f of the conduction-electron spins is much smaller than that of the localized electron spins. We use Gilbert's expression as the magnetic damping term, namely, the second term of Eq. (11). In Ref. 6, Bloch's expression was used, while Gilbert's expression is appropriate for describing the magnetic damping for the strongly coupled spins.[27] We assume that the torque by the exchange interaction of $\mathbf{M}_f$ is expressed as

$$\mathbf{T}=\mathbf{M}\times\lambda\mathbf{M}_f, \tag{12}$$

where λ is the molecular field coefficient, and $\mathbf{T}$, which had been neglected in Ref. 6, is essential for our discussion. In the case of $\mathbf{T}=0$, Eq. (11) is identical to Eq. (1) by taking $\gamma=\gamma_F$ and $G=G_F$, namely, the dynamics of the magnetization are determined only by the nature of the localized electron spins. The dynamics of $\mathbf{M}_f$ are assumed to be expressed as

$$\frac{d\mathbf{M}_f}{dt}=-\gamma_f\mathbf{M}_f\times\lambda\mathbf{M}-\frac{\mathbf{M}_f-\chi_f\lambda\mathbf{M}}{\tau_f}-\frac{\mathbf{J}_f}{d_{\rm Py}}. \tag{13}$$

Here, γ_f, χ_f, and τ_f are the gyromagnetic ratio, Pauli paramagnetic susceptibility, and the spin-relaxation time for the conduction electron in the Py layer, respectively. $\mathbf{J}_f$ is the current density of the spin magnetic moment diffusing out of the Py layer at the Py/Cu interface. We do not treat the spatial variation of $\mathbf{M}_f$ inside the Py layer. The molecular field of the exchange interaction $\lambda\mathbf{M}$ is taken only into account as the effective magnetic field. The dynamics and the transport of $\mathbf{m}_p$ are well described by the Bloch-Torrey equation,[6,28]

$$\frac{\partial\mathbf{m}_p}{\partial t}=-\gamma_p\mathbf{m}_p\times\mathbf{H}-\frac{\mathbf{m}_p-\chi_p\mathbf{H}}{\tau_p}+D_p\frac{\partial^2}{\partial Z^2}(\mathbf{m}_p-\chi_p\mathbf{H}). \tag{14}$$

γ_p, χ_p, and τ_p denote the same as those of $\mathbf{M}_f$. D_p is the diffusion coefficient for the conduction electron in the Cu layer. We neglect any other magnetic field acting on $\mathbf{m}_p$ except for $\mathbf{H}$. The spatial variation of $\mathbf{m}_p$ depends only on the Z direction and is uniform in the X-Y plane. The spin diffusion at the Py/Cu interface is taken into account as the boundary condition at $Z=0$. Assuming that there is no spin relaxation at this interface, and neglecting the small difference between γ_f and γ_p, the boundary condition is expressed as[6]

$$\mathbf{J}_f=\mathbf{J}_p=\Gamma\left(\frac{\mathbf{M}_f-\chi_f\lambda\mathbf{M}}{\chi_f}-\frac{\mathbf{m}_p-\chi_p\mathbf{H}}{\chi_p}\right), \tag{15}$$

where Γ characterizes the rate of the spin diffusion at this interface. $\mathbf{J}_p$ is the current density of the spin magnetic moment inside the Cu layer, and is given as

$$\mathbf{J}_p=-D_p\frac{\partial}{\partial Z}(\mathbf{m}_p-\chi_p\mathbf{H}). \tag{16}$$

The spin relaxation at the Cu/Pt interface or the surface of the Cu layer is also taken into account as the boundary condition at $Z=d_{\rm Cu}$, which is given by[28,29]

$$\mathbf{J}_p=\alpha_S(\mathbf{m}_p-\chi_p\mathbf{H}). \tag{17}$$

Here, α_S characterizes the rate of the spin relaxation at the Cu/Pt interface or the Cu surface.

We analyze $\mathbf{T}$ on the linear approximation using Eqs. (11)–(17). On resonance in FMR, $\mathbf{h}$ excites the small precession of $\mathbf{M}$ around the equilibrium direction, which is expressed the same as that in Eq. (3). The precession of $\mathbf{M}$ drives $\mathbf{M}_f$ by the exchange interaction, which is given as

$$\mathbf{M}_f(t)=\chi_f\lambda\mathbf{M}(t)+\delta\mathbf{M}_f e^{-i\omega t}. \tag{18}$$

Here, the first and the second terms are the instantaneous equilibrium magnetization and the induced nonequilibrium magnetization, respectively. The induced nonequilibrium magnetization of $\mathbf{M}_f$ diffuses from the Py to the Cu layer as the spin current described in Eq. (15), and the nonequilibrium magnetization of $\mathbf{m}_p$ is built up inside the Cu layer, which is expressed as

$$\mathbf{m}_p(Z,t)=\chi_p\mathbf{H}+\delta\mathbf{m}_p(Z)e^{-i\omega t}. \tag{19}$$

The first and the second terms are the thermal equilibrium magnetization and the induced nonequilibrium magnetization, respectively. We take the linear combination of the rightward and the leftward propagating wave as a solution of $\delta\mathbf{m}_p(Z)$, which is given by

$$\delta\mathbf{m}_p(Z)=\sum_{j=+,-,z}(\delta m_{pj}^R e^{ik_{pj}Z}+\delta m_{pj}^L e^{-ik_{pj}Z})\hat{\mathbf{e}}_{pj}. \tag{20}$$

Here, $\hat{\mathbf{e}}_{pj}$ is the polarization vector of the precession given as $\hat{\mathbf{e}}_{p\pm}=[\hat{\mathbf{x}}\mp i(\cos\beta)\hat{\mathbf{y}}\mp i(\sin\beta)\hat{\mathbf{z}}]/\sqrt{2}$ and $\hat{\mathbf{e}}_{pz}=-(\sin\beta)\hat{\mathbf{y}}+(\cos\beta)\hat{\mathbf{z}}$, with $\beta\equiv\theta-\theta_H$. Substituting Eqs. (19) and (20) into Eq. (14), one obtains the propagation constant k_{pj} given as

$$k_{p\pm}^2=i(\omega\pm\omega_p)/D_p-l_p^{-2}, \tag{21}$$

$$k_{pz}^2=i\omega/D_p-l_p^{-2}. \tag{22}$$

Here, ω_p is the Larmor frequency defined as $\omega_p\equiv\gamma_p H$, and l_p is the spin-diffusion length for the Cu layer defined as $l_p\equiv\sqrt{D_p\tau_p}$. Equations (21) and (22) mean that the wavelength and the attenuating length of the propagating spin density depend on H, l_p, and the polarization of the precession. Such a propagating mode is inherent for the transport of the precessional spin of the conduction electron,[30,31] and which is different from the usual spin transport, such as the current perpendicular-to-plane magnetoresistance, for which the characteristic length is l_p.[32] While, in the case of

$$[(\omega\pm\omega_p)\tau_p]^2\ll 1 \quad\text{and}\quad (\omega\tau_p)^2\ll 1, \tag{23}$$

$k_{pj}^2=-l_p^{-2}$ is approximately obtained from Eqs. (21) and (22).[33] In a further analysis, we assume that Eq. (23) is satisfied for the Cu layer, for simplicity. δm_{pj}^R and δm_{pj}^L are determined from Eqs. (15)–(17) using Eqs. (18)–(20), and the relation between $\delta\mathbf{m}_p(0)$ and $\delta\mathbf{M}_f$ is obtained. Using its relations with Eqs. (15), (18), and (19), we obtain the following relation:

$$\mathbf{J}_f=(\Gamma_{\mathrm{eff}}/\chi_f)\delta\mathbf{M}_f e^{-i\omega t}. \tag{24}$$

Here, Γ_{eff} is the effective rate of the interfacial spin diffusion modified by the dynamics and transport of $\mathbf{m}_p$, which is defined as

$$\Gamma_{\mathrm{eff}}^{-1}\equiv\Gamma^{-1}+\left[\chi_p\left(\frac{D_p}{l_p}\right)\frac{(D_p/l_p)\tanh(d_{\mathrm{Cu}}/l_p)+\alpha_S}{(D_p/l_p)+\alpha_S\tanh(d_{\mathrm{Cu}}/l_p)}\right]^{-1}. \tag{25}$$

Equation (24) means that the nonequilibrium magnetization induced by the precession of $\mathbf{M}$ is lost from the Py layer on resonance of FMR. Substituting Eqs. (18) and (24) into Eq. (13) and introducing

$$\delta M_{(f)\pm}\equiv\delta M_{(f)x}\pm i\,\delta M_{(f)y}, \tag{26}$$

one obtains

$$\delta M_{f\pm}=\frac{i\tau_{\mathrm{eff}}}{1-i(\omega\pm\omega_f)\tau_{\mathrm{eff}}}\omega\chi_f\lambda\,\delta M_{\pm} \tag{27}$$

and $\delta M_{fz}=0$. Here, ω_f is defined as $\omega_f\equiv\gamma_f\lambda M_S$, and τ_{eff} is the effective spin-relaxation time for the conduction electron in the Py layer, which is also defined as

$$1/\tau_{\mathrm{eff}}\equiv 1/\tau_f+\Gamma_{\mathrm{eff}}/\chi_f d_{\mathrm{Py}}. \tag{28}$$

ω_f is considered to be quite large for an ordinary FM, such as Py, so that $\omega/\omega_f\ll 1$ is sufficiently satisfied, and we assume

$$(\omega_f\tau_{\mathrm{eff}})^{-2}\ll 1. \tag{29}$$

Taking the leading order of the real and the imaginary parts of Eq. (27) on this assumption, Eq. (27) becomes

$$\delta M_{f\pm}=(\mp 1/\omega_f+i/\omega_f^2\tau_{\mathrm{eff}})\omega\chi_f\lambda\,\delta M_{\pm}. \tag{30}$$

Using Eqs. (12), (18), (26), and (30), one obtains the following expression for $\mathbf{T}$:

$$\mathbf{T}=\frac{\chi_f\lambda}{\gamma_f}\frac{d\mathbf{M}}{dt}-\frac{\chi_f\tau_{\mathrm{eff}}^{-1}}{(\gamma_f M_S)^2}\mathbf{M}\times\frac{d\mathbf{M}}{dt}. \tag{31}$$

The first and the second terms are the additional terms of the gyromagnetic ratio (the so-called g shift), and Gilbert damping, respectively. Substituting Eq. (31) into Eq. (11), one obtains an LLG equation, which is the same as Eq. (1), by taking $\gamma=\gamma_F$ and

$$G=G_F+\chi_f/\tau_{\mathrm{eff}}. \tag{32}$$

Here, we used $\chi_f\lambda\ll 1$ and $\gamma_F/\gamma_f\simeq 1$, which are satisfied in an ordinary FM. γ is not influenced by the dynamics and the transport of the conduction-electron spins, so that it is independent of d_{Py} and d_{Cu}. In the case of $G_F=0$ and $\tau_{\mathrm{eff}}=\tau_f$, Eq. (32) is in accord with the previous theory for Gilbert damping of bulk FM based on the s-d model.[34] Using Eqs. (25), (28), and (32), G is rewritten as

$$G=G_{\mathrm{Py}}+G', \tag{33}$$

where G_{Py} is the Gilbert damping coefficient for the bulk Py, which is defined as $G_{\mathrm{Py}}\equiv G_F+\chi_f/\tau_f$, and G' is the interfacial contribution of G, which is defined as

$$G'\equiv\Gamma_{\mathrm{eff}}/d_{\mathrm{Py}}. \tag{34}$$

Here, χ_f was canceled out, so that G' is independent of the properties inside the Py layer. G' increases with decreasing d_{Py}, so that G' is not negligible for a very thin Py layer. In the case that d_{Cu} is sufficiently small, Eq. (34) becomes

$$G' = [\Gamma^{-1} + (\chi_p \alpha_S)^{-1}]^{-1}/d_{\mathrm{Py}}, \tag{35}$$

taking $d_{\mathrm{Cu}} \ll l_p$ in Eq. (25). The magnitude of G' is governed by the rate of the spin diffusion at the Py/Cu interface and the relaxing rate of spin at the Cu/Pt interface or the Cu surface. If the spin relaxation at the Cu/Pt interface is infinitely strong, namely $\alpha_S^{-1} \to 0$, Eq. (35) becomes $G' = \Gamma/d_{\mathrm{Py}}$. This means that the Cu layer in contact with the Pt layer operates as a spin sink. In the case of no spin relaxation at the Cu surface, namely $\alpha_S = 0$, G' becomes zero, because the spin diffusion from the Py to the Cu layer is balanced on that from the Cu to the Py layer. On the other hand, in the case of $d_{\mathrm{Cu}} \gg l_p$, G' is expressed as

$$G' = [\Gamma^{-1} + (\chi_p D_p/l_p)^{-1}]^{-1}/d_{\mathrm{Py}}.$$

The spin relaxation at the Cu/Pt interface or the Cu surface is not operative in this regime because spin cannot diffuse beyond l_p inside the Cu layer. Instead of α_S, G' is influenced by the bulk spin relaxation of Cu, namely, τ_p involved in l_p.

In order to quantitatively examine this model, the calculated G vs d_{Cu} was fitted to the experimental one using Eqs. (25), (33), and (34). In the fitting, we took $G_{\mathrm{Py}} = 0.69 \times 10^8\ \mathrm{s}^{-1}$, which corresponded to the value of G for Cu/Py/Cu (100 Å) film, and $\chi_p \simeq 9.8 \times 10^{-7}$ in cgs unit. The value of χ_p was estimated from $\chi_p = \mu_B^2 3n/2E_F$ on the free-electron model using an electron density $n \simeq 8.5 \times 10^{22}\ \mathrm{cm}^{-3}$ and a Fermi energy $E_F = 7$ eV for Cu.[35] Furthermore, α_S for the Cu surface was taken to be zero in the fitting for Cu/Py/Cu films, because α_S for the Cu surface is considered to be negligibly small.[36] The remaining unknown parameters are D_p, l_p, Γ, and α_S for the Cu/Pt interface. The values of D_p and l_p can be determined almost independently from the fitting. While, the value of Γ and α_S for the Cu/Pt interface cannot be obtained uniquely, because of the various combinations of the values of Γ and α_S for the Cu/Pt interface that are allowed for the best fitting to G vs d_{Cu} for Cu/Py/Cu/Pt films. An example of the fitting is shown in Fig. 6 with the solid and the broken lines for Cu/Py/Cu/Pt and Cu/Py/Cu films, respectively. The fitting shown in Fig. 6 was performed taking $\alpha_S^{-1} \to 0$ for the Cu/Pt interface and regarding D_p, l_p, and Γ as adjustable parameters. The calculated G vs d_{Cu} is well fitted to the experimental data. From this fitting, the values of D_p, l_p, and Γ were obtained to be $120 \pm 20\ \mathrm{cm}^2/\mathrm{s}$, 2000 ± 500 Å, and 30 ± 5 cm/s, respectively. In the case of a fitting taking $\Gamma^{-1} \to 0$ and adjusting the values of D_p, l_p, and α_S for the Cu/Pt interface, we obtained the result of the fitting and the values of D_p and l_p were the same as those in Fig. 6, and α_S for the Cu/Pt interface was $3 \pm 0.5 \times 10^7$ cm/s. Thus, although we cannot obtain the exact values of Γ and α_S for the Cu/Pt interface, they are restricted as $\Gamma \geqslant 30$ cm/s and $\alpha_S \geqslant 3 \times 10^7$ cm/s for the Cu/Pt interface for the best fitting. D_p for the bulk-Cu on the free-electron model is estimated to be $\simeq 160\ \mathrm{cm}^2/\mathrm{s}$ from $D_p = v_p \Lambda_p/3$ using the Fermi velocity $v_p \simeq 1.6 \times 10^8$ cm/s and the mean free path $\Lambda_p \simeq 300$ Å.[35] The typical reported values of l_p are $\simeq 4500$ Å at 4.2 K in Ref. 25 or $\simeq 3500$ Å at RT in Ref. 26. The values of D_p and l_p obtained from the fitting are consistent with the above referred values, taking into consideration the influence on D_p and l_p of the ordinary and the spin-orbit scattering by defects and phonon.[37] From the kinetic argument based on the free-electron model, α_S is considered to be expressed as $\alpha_S = v_p \epsilon/2(1-\epsilon)$.[28,29] Here, ϵ is the probability of the spin-flip reflection at an interface or a surface. For the Cu/Pt interface, $\epsilon \geqslant 0.3$ is estimated from $\alpha_S \geqslant 3 \times 10^7$ cm/s using this relation and $v_p \simeq 1.6 \times 10^8$ cm/s. The lower limit of ϵ is considered to be evaluated roughly from σ_r/σ_{sf}, where σ_r and σ_{sf} are the cross section of the resistivity and the spin-flip scattering for an impurity atom in a host metal, respectively. σ_r/σ_{sf} for a Pt atom in Cu is evaluated to be $\simeq 0.1$,[25,38] so that $\epsilon \geqslant 0.3$ is a reasonable estimate. $\Gamma \geqslant 30$ cm/s at the Py/Cu interface in our films is also roughly consistent with $\Gamma \simeq 15$ cm/s estimated from the best value of $\Gamma'/\chi_p = 1.5 \times 10^7$ cm/s in Ref. 6 taking $\Gamma' = \Gamma$ and $\chi_p \simeq 9.8 \times 10^{-7}$. In addition, according to a microscopic calculation of Γ,[39] Γ for NM/NM tunnel junction is given as $\Gamma = \xi(\mu_B/e)^2 R^{-1}$, where e is the electron charge and R is the junction resistance at the NM/NM interface. If this relation is valid for a metallic contact of FM/NM in our case, $\Gamma \geqslant 30$ cm/s leads to $R \leqslant 1\ \mathrm{f}\Omega\ \mathrm{m}^2$ from this relation, which is also consistent with $R = 0.5\ \mathrm{f}\Omega\ \mathrm{m}^2$ for the sputtered Py/Cu/Py films.[40]

This model also agrees with the experimental data, except for the fitting of G vs d_{Cu}. It is expected from Eq. (35) that the difference of ΔH_{pp} between Cu/Py/Cu/Pt and Cu/Py/Cu films increases as d_{Py} decreases in the thinner regime of d_{Cu} as in Fig. 3(b). In addition, this model provides a natural explanation for the experimental fact that G for Cu/Py/Cu/Cu/Pt films was not enhanced. For Cu/Py/Cu/Cu/Pt films, the spin diffusion is disturbed by the low conductive regime that possibly exists in the middle of the Cu spacer layer, so that G is considered to be same as that for Cu/Py/Cu films. Silsbee *et al.* have also reported the similar influence of oxidation or contamination at the interface on the transmitted signal of CESR for their bilayer.[6]

The assumption of Eq. (23) has to be self-consistently satisfied with $\tau_p \simeq 3 \times 10^{-12}$ s estimated from D_p and l_p obtained from the fitting. In the case of $\tau_p \simeq 3 \times 10^{-12}$ s, the approximation of Eq. (23) is crude near $\theta_H = 0°$, because the magnitude of H becomes very large nearby this angle as shown in the insets of Figs. 5(a) and 5(b). However, this is considered to be almost ineffective for the fitting in Fig. 6, since the experimental G is mostly determined by the magnitude of ΔH_{pp} near $\theta_H = 90°$, as shown in Figs. 5(a) and 5(b). A check of the validity of Eq. (29) is also required because Eq. (29) is essential for deriving Eq. (31) as Gilbert type damping.[34] ω_f is considered to be identical to $2JS/\hbar$, where J and S are the constants of the s-d exchange and the average spin of the localized d-electron moment, respectively. Taking $J = 0.4$ eV from Ref. 41 and $S = 0.5$, ω_f is estimated to be $\simeq 6 \times 10^{14}\ \mathrm{s}^{-1}$. τ_f is estimated to be $\simeq 3 \times 10^{-14}$ s from the spin-diffusion length for Py $l_f \simeq 55$ Å in Ref. 40, assuming the diffusion coefficient for Py $D_f \simeq 10\ \mathrm{cm}^2/\mathrm{s}$. The value of $\Gamma_{\mathrm{eff}}/\chi_f d_{\mathrm{Py}}$ used in the fitting is found to be less than about $1 \times 10^{14}\ \mathrm{s}^{-1}$ by assuming $\chi_p = \chi_f$. Thus, Eq. (29) is satisfied enough in the fitting.

We comment on the validity of using Eq. (13). In Ref. 6, Silsbee *et al.* had originally taken into account the spatial variation of $\mathbf{M}_f$ using a Bloch-Torry equation, as performed for the Cu layer. In such a case, the spatial variation of $\mathbf{M}_f$ is characterized by the propagation constant for Py k_{fj}, which is defined by changing the index p into f in Eqs. (21) and (22) and becomes $k_{fj}^2 \simeq i\omega_f/D_f$ with $\omega_f \gg \omega$, τ_f^{-1}. This means that the propagation of $\mathbf{M}_f$ is heavily damped in the range of $\sqrt{2D_f/\omega_f}$, not by the bulk spin relaxation but by the exchange interaction. In the case of $d_{\mathrm{Py}} \ll \sqrt{2D_f/\omega_f}$, the spatial variation of $\mathbf{M}_f$ can be neglected, and Eq. (13) is satisfied. Taking $\omega_f \simeq 6\times 10^{14}$ s^{-1} and $D_f \simeq 10$ cm^2/s, $\sqrt{2D_f/\omega_f}$ is estimated to be $\simeq 20$ Å. This length is comparable to or smaller than not only d_{Py} but also the mean free path for Py. Such a rapid variation of magnetization cannot be described by the Bloch-Torry equation.[28] Therefore, the validity of Eq. (13) cannot be fully justified. Further experimental and theoretical studies are needed for clarifying the validity of Eq. (13).

Our experimental result and its interpretation agreed with the microscopic theories taking into account spin current generated by the precession of magnetization in NM/FM/NM films.[42,43] On the other hand, Berger theoretically suggested that G was enhanced in FM/NM/FM films,[1,4] and this was also confirmed recently in Fe/Au/Fe films.[44] It is unclear whether the mechanism of the enhancement of G for Fe/Au/Fe film is essentially different from that for our films. It is likely that the roll of a thick Fe layer for Fe/Au/Fe film is the same as that of Pt layer for ours, because the relaxation for precessional spin is strongly operative in a sufficiently thick FM film because of the large s-d exchange, as described above.[6,43] In addition, a phenomenological model describing spin dynamics and transport for FM was also suggested recently, which was somewhat different from the model used in this paper and took into account not only charge and spin current but also the cross spin relaxation between conduction and localized spin system.[45] Comparison between these other reports and our result is further subject.

VI. SUMMARY

FMR was measured for Cu/Py (d_{Py})/Cu (d_{Cu})/Pt films with various d_{Cu} and d_{Py} in order to clarify the effect of spin diffusion driven by the precession of magnetization on Gilbert damping. ΔH_{pp} for Cu/Py/Cu/Pt films was very large at $d_{\mathrm{Cu}}=0$ Å and decreased remarkably at $d_{\mathrm{Cu}}=30$ Å. Above $d_{\mathrm{Cu}}=30$ Å, it decreased gradually with increasing d_{Cu} in the anomalously wide range of d_{Cu}. This trend became more remarkable with decreasing d_{Py}. The out-of-plane angular dependence of FMR for Cu/Py (30 Å)/Cu (d_{Cu})/Pt (0, 50 Å) films was measured and analyzed using an LLG equation taking into account the local variation of $4\pi M_{\mathrm{eff}}$. The value of G obtained from the analysis for Cu/Py/Cu/Pt films was about twice as large as that for Cu/Py/Cu films even at $d_{\mathrm{Cu}}=100$ Å and decreased gradually as d_{Cu} increased. At $d_{\mathrm{Cu}}=2000$–3000 Å, G for Cu/Py/Cu/Pt and Cu/Py/Cu films became the same value. We also discussed the influence of the spin diffusion driven by the precession of magnetization in FMR on G using the model proposed in the past. The calculated G vs d_{Cu} was well fitted to the experimental one, and the model explained other features of the experimental results.

ACKNOWLEDGMENTS

We acknowledge very fruitful discussions with A. Fert, Y. Suzuki, and Y. Tserkovnyak. We also thank Y. Tserkovnyak, A. Brataas, and G. E. W. Bauer for sending their preprint. This work had been supported by the Mitsubishi foundation, the Storage Research Consortium, CREST of JST (Japan Science and Technology), and Grants-in-Aid for Scientific Research from the Ministry of Education, Science, Sports and Culture of Japan.

*Present address: Nihon University, College of Engineering, Koriyama, Fukushima, Japan.

[1] L. Berger, Phys. Rev. B **54**, 9353 (1996).

[2] J.C. Slonczewski, J. Magn. Magn. Mater. **159**, L1 (1996).

[3] M. Tsoi, A.G.M. Jansen, J. Bass, W.-C. Chiang, M. Seck, V. Tsoi, and P. Wyder, Phys. Rev. Lett. **80**, 4281 (1998); J.Z. Sun, J. Magn. Magn. Mater. **202**, 157 (1999); J.A. Katine, F.J. Albert, R.A. Buhrman, E.B. Myers, and D.C. Ralph, Phys. Rev. Lett. **84**, 3149 (2000); J. Grollier, V. Cros, A. Hamzic, J.M. George, H. Jaffres, A. Fert, G. Faini, J. Ben Youssef, and H. Legall, Appl. Phys. Lett. **78**, 3663 (2001).

[4] L. Berger, Phys. Rev. B **59**, 11 465 (1999); L. Berger, J. Appl. Phys. **90**, 4632 (2001).

[5] A. Jánossy and P. Monod, Solid State Commun. **18**, 203 (1976).

[6] R.H. Silsbee, A. Jánossy, and P. Monod, Phys. Rev. B **19**, 4382 (1979).

[7] P.D. Sparks and R.H. Silsbee, Phys. Rev. B **35**, 5198 (1987).

[8] Z. Frait and D. Fraitová, in *Spin Waves and Magnetic Excitations*, edited by A.S. Borovik-Romanov and S.K. Sinha (North-Holland, Amsterdam, 1988), Pt. 2, Chap. 1, p. 1; B. Heinrich and J.F. Cochran, Adv. Phys. **42**, 523 (1993).

[9] F. Schreiber, J. Pflaum, Z. Frait, Th. Mühge, and J. Pelzl, Solid State Commun. **93**, 965 (1995).

[10] B. Heinrich, K.B. Urquhart, A.S. Arrott, J.F. Cochran, K. Myrtle, and S.T. Purcell, Phys. Rev. Lett. **59**, 1756 (1987); Z. Celinski and B. Heinrich, J. Appl. Phys. **70**, 5935 (1991); M. Farle, J. Lindner, and K. Baberschke, J. Magn. Magn. Mater. **212**, 301 (2000).

[11] W. Platow, A.N. Anisimov, G.L. Dunifer, M. Farle, and K. Baberschke, Phys. Rev. B **58**, 5611 (1998).

[12] S. Mizukami, Y. Ando, and T. Miyazaki, Jpn. J. Appl. Phys., Part 1 **40**, 580 (2001).

[13] S. Mizukami, Y. Ando, and T. Miyazaki, J. Magn. Magn. Mater. **226-230**, 1640 (2001).

[14] V. Kamberský, Can. J. Phys. **48**, 2906 (1970); V. Korenman and R.E. Prange, Phys. Rev. B **6**, 2679 (1972); L. Berger, J. Phys. Chem. Solids **38**, 1321 (1977).

[15] S. Mizukami, Y. Ando, and T. Miyazaki, J. Magn. Magn. Mater. **239**, 42 (2002).

[16] A.Z. Maksymowicz and K.D. Leaver, J. Phys. F: Met. Phys. **3**,

1031 (1973); A.A. Hussain, Physica B **162**, 321 (1990).
[17] C. Chappert, K. Le Dang, P. Beauvillain, H. Hurdequint, and D. Renard, Phys. Rev. B **34**, 3192 (1986).
[18] T.D. Rossing, J. Appl. Phys. **34**, 995 (1963).
[19] J.K. Blum and W. Göpel, Ber. Bunsenges. Phys. Chem. **82**, 329 (1978); J.L. Bubendorff, J. Pflaum, E. Huebner, D. Raiser, J.P. Bucher, and J. Pelzl, J. Magn. Magn. Mater. **165**, 199 (1997).
[20] R.D. McMichael, M.D. Stiles, P.J. Chen, and W.F. Egelhoff, Jr., J. Appl. Phys. **83**, 7037 (1998); R. Arias and D.L. Mills, Phys. Rev. B **60**, 7395 (1999).
[21] D. Bastian and E. Biller, Phys. Status Solidi A **35**, 465 (1976).
[22] J.W. Smits, H.A. Algra, U. Enz, and R.P. van Stapele, J. Magn. Magn. Mater. **35**, 89 (1983).
[23] C.E. Patton, Z. Frait, and C.H. Wilts, J. Appl. Phys. **46**, 5002 (1975); D. Bastian and E. Biller, Phys. Status Solidi A **35**, 113 (1976).
[24] S.S.P. Parkin, R. Bhadra, and K.P. Roche, Phys. Rev. Lett. **66**, 2152 (1991); P. Bruno and C. Chappert, *ibid.* **67**, 1602 (1991); R. Coehoorn, A. De Veirman, and J.P.W.B. Duchateau, J. Magn. Magn. Mater. **121**, 266 (1993).
[25] Q. Yang, P. Holody, S.-F. Lee, L.L. Henry, R. Loloee, P.A. Schroeder, W.P. Pratt, Jr., and J. Bass, Phys. Rev. Lett. **72**, 3274 (1994).
[26] F.J. Jedema, A.T. Fillip, and B.J. van Wees, Nature (London) **410**, 345 (2001).
[27] R.K. Wangsness, Phys. Rev. **104**, 857 (1956); V. Kamberský and C.E. Patton, Phys. Rev. B **11**, 2668 (1975).
[28] M.B. Walker, Phys. Rev. B **3**, 30 (1971).
[29] M.R. Menard and M.B. Walker, Can. J. Phys. **52**, 61 (1974).
[30] M. Johnson and R.H. Silsbee, Phys. Rev. B **37**, 5312 (1988).
[31] D.H. Hernando, Yu.V. Nazarov, A. Brataas, and G.E.W. Bauer, Phys. Rev. B **62**, 5700 (2000).
[32] T. Valet and A. Fert, Phys. Rev. B **48**, 7099 (1993).
[33] G.W. Graham and R.H. Silsbee, Phys. Rev. B **22**, 4184 (1980).
[34] B. Heinrich, D. Fraitová, and V. Kamberský, Phys. Status Solidi **23**, 501 (1967).
[35] C. Kittel, *Introduction to Solid State Physics* (Wiley, New York, 1996).
[36] S. Schultz and C. Latham, Phys. Rev. Lett. **15**, 148 (1965); A. Stesmans, J. van Meijel, and S.P. Braim, Phys. Rev. B **19**, 5470 (1979).
[37] R.J. Elliott, Phys. Rev. **96**, 266 (1954); F. Beuneu and P. Monod, Phys. Rev. B **13**, 3424 (1976); P. Monod and F. Beuneu, *ibid.* **19**, 911 (1979).
[38] A. Fert, J.-L. Duvail, and T. Valet, Phys. Rev. B **52**, 6513 (1995); P. Monod and S. Schultz, J. Phys. (Paris) **43**, 393 (1982); J. Cottet, Ph. D. thesis, Université de Genève, Geneva, 1970.
[39] G.G. Khaliullin and M.G. Khusainov, Zh. Éksp. Teor. Fiz. **86**, 187 (1984) [Sov. Phys. JETP **59**, 106 (1984)].
[40] S.D. Steenwyk, S.Y. Hsu, R. Loloee, J. Bass, and W.P. Pratt, Jr., J. Magn. Magn. Mater. **170**, L1 (1997).
[41] A. Fert and I.A. Campbell, J. Phys. F: Met. Phys. **6**, 849 (1976).
[42] Y. Tserkovnyak, A. Brataas, and G.E.W. Bauer, Phys. Rev. Lett. **88**, 117601 (2002).
[43] Y. Tserkovnyak (private communication).
[44] R. Urban, G. Woltersdorf, and B. Heinrich, Phys. Rev. Lett. **87**, 217204 (2001).
[45] C. Heide, Phys. Rev. Lett. **87**, 197201 (2001); Phys. Rev. B **65**, 054401 (2001).